SPANDIDOS PUBLICATIONS

Expression of BRCC3, a novel cell cycle regulated molecule, is associated with increased phospho-ERK and cell proliferation

HOWARD E. BOUDREAU[1,2], CONSTANTINOS G. BROUSTAS[1], PRAFULLA C. GOKHALE[1], DEEPAK KUMAR[1], RAJSHREE R. MEWANI[1], JANICE D. RONE[3], BASSEM R. HADDAD[3] and USHA KASID[1,2]

[1]Departments of Radiation Medicine, [2]Biochemistry and Molecular and Cellular Biology, and [3]Oncology, Lombardi Comprehensive Cancer Center, Georgetown University Medical Center, Washington DC 20057, USA

Received June 30, 2006; Accepted August 24, 2006

Abstract. Raf-1 protein serine/threonine kinase plays an important role in ERK signal transduction pathway of cell survival and proliferation. Raf-induced transcriptional changes are dependent on phosphorylation/activation of ERK. However, regulation of phospho-ERK (p-ERK) via Raf transcriptome is as yet unknown. We report the initial characterization of BRCC3, a novel gene discovered previously by mRNA expression profiling in MDA-MB 231 human breast cancer cells treated with Raf antisense oligonucleotide. BRCC3 is localized at human chromosome 5q12.1. BRCC3 open reading frame consists of 529 amino acids, coding for an approximate 60-kDa predominantly membrane-associated protein. Expression levels of BRCC3 mRNA and protein are high during G2/M phase of the cell cycle in breast cancer cells. Treatment of MDA-MB 231 cells with Raf-1 siRNA resulted in decreased expression of Raf-1, BRCC3 and p-ERK, but not B-Raf. Transient or stable expression of the epitope-tagged BRCC3 cDNA was associated with increased p-ERK in three different cell lines. Consistently, BRCC3 siRNA treatment of MDA-MB 231 cells caused decreased expression of BRCC3 and p-ERK. Furthermore, exogenous BRCC3 expression was associated with a delay in etoposide-induced cell death and an increase in cell proliferation. These findings demonstrate that BRCC3 is a novel effector of Raf-1, and implicate a role of BRCC3 in modulation of p-ERK, cell survival and proliferation.

Introduction

Raf-1 is a cytosolic serine/threonine protein kinase involved in cell growth, proliferation, differentiation, and survival (1-3). There are several upstream activators of Raf-1 such as Ras, B-Raf, PI(3)K, PKC and integrin, thereby making Raf-1 a central convergent point for multiple signaling pathways (4-6). Once activated by external stimuli such as growth factors or ionizing radiation, Raf-1 activates mitogen-activated protein kinase kinase (MEK) and extracellular signal-regulated kinase (ERK), the predominant downstream effectors of the classical MAPK pathway (Ras>Raf>MEK>ERK) (4,7-9). Dephosphorylation of the inhibitory phosphorylation site of Raf-1 (serine-259) by protein serine/threonine phosphatase 2A has been shown to activate the Raf-1>MEK>ERK pathway (10). Phosphorylation and activation of ERK is an important link between several growth factor receptors at the cell membrane and transcriptional factors in the nucleus (11-13). Consistently, Raf-1 transformed cells exhibit changes in transcription of several genes involved in cell proliferation and invasion, and ERK activity seems to be essential for transcriptional changes induced by Raf-1 (14-16). Raf-1 may function in a kinase-independent manner. In the latter context, it seems to regulate apoptotic signals ASK1 and MST2 and cell motility via Rok-α (17-19). Raf-1 has been also shown to cross-talk with other pathways, suggesting the involvement of as yet unknown effectors of Raf-1 (20).

Raf-1 is an important determinant of resistance of tumors to radiation and chemotherapeutic drugs (21,22). Antisense oligonucleotide, siRNA, and small molecule strategies to inhibit Raf-1 have been successfully used to achieve anti-tumor and radio-/chemo-sensitization effects *in vivo* (23-26). Several clinical trials targeting Raf-1 have been reported (27-33). The investigation of the changes in gene expression via inhibition of Raf-1 may identify new molecules and advance our understanding of the mechanism(s) of cell survival, proliferation, or resistance of tumor cells to standard cancer therapies. Towards this goal, we analyzed the mRNA expression profile of MDA-MB231 breast cancer cells treated with c-*raf*-1 antisense oligonucleotide. Raf-1 inhibition via antisense oligonucleotide resulted in a concomitant inhibition of the mRNA expression of a novel gene BRCC3 (breast cancer cell 3) (GenBank accession no. AF220062). BRCC3 cDNA sequence is similar to XTP8 (GenBank accession no. AF490257), human gene 8 transactivated by hepatitis B virus (HBV) X oncoprotein (HBX). Interestingly, HBX has been shown to activate the ERK and PI(3)K pathways and has been implicated in HBV-mediated hepatocellular carcinoma (34-36).

The main objectives of this study were to investigate a relationship between BRCC3 and phospho-ERK (p-ERK),

Correspondence to: Dr Usha Kasid, E208 Research Building, Georgetown University Medical Center, 3970 Reservoir Road, NW, Washington DC 20057, USA
E-mail: kasidu@georgetown.edu.

Keywords: BRCC3, Raf-1, phospho-ERK, cell viability and proliferation

and to determine a biological role of BRCC3. We report, for the first time, a correlation between inhibition of Raf-1 and decreased expression of BRCC3 protein. Modulation of the BRCC3 level by either cDNA expression or siRNA treatment resulted in a concomitant increase or decrease of p-ERK, respectively. BRCC3 cDNA expression was associated with a delay in etoposide-induced cell death and an increase in cell proliferation. Present findings reveal a potential link between BRCC3 and positive regulation of the ERK pathway.

Materials and methods

Cell culture. MCF-7 human breast cancer cells were obtained from the American Type Culture Collection (Rockville, MD). All other cell lines [HEK-293T, COS-1, HeLa, human breast cancer cells (MDA-MB 231 and MDA-MB 435), human prostate cancer cells (PC-3)] were obtained from the Tissue Culture Shared Resource facility of the Lombardi Cancer Center, Georgetown University Medical Center. All cell lines with the exception of MDA-MB 231 were grown in Dulbecco's minimum essential medium (DMEM) supplemented with 10% heat-inactivated fetal bovine serum (FBS) and 25 μg/ml gentamycin, all obtained from Invitrogen/Gibco (Carlsbad, CA). MDA-MB-231 human breast cancer cells were grown in Iscove's minimum essential medium (IMEM) from Biofluids (Camarillo, CA) supplemented with 10% heat-inactivated FBS, 2 mM L-glutamine, and 100 mg/ml penicillin/streptomycin (Biofluids). All cells were cultured in a humidified atmosphere of 5% CO_2 and 95% air at 37˚C.

Antibodies and chemicals. Rabbit polyclonal anti-BRCC3 antiserum was custom generated by Zymed Laboratories Inc. (San Francisco, CA) against a BRCC3-specific peptide PFQPFRTRSFRM-(C), the last cysteine was added for conjugation purposes. The following antibodies and chemicals were obtained commercially: anti-Myc (9E10) monoclonal, anti-Raf-1 polyclonal (C-12), anti-B-Raf polyclonal, and anti-cyclin B1 monoclonal antibodies (Santa Cruz Biotechnology, Santa Cruz, CA); anti-phospho-p44/p42 MAPK (E10), anti-p44/p42 MAPK, and anti-caspase-3 polyclonal antibodies (Cell Signaling, Beverly, MA); anti-GAPDH polyclonal antibody (Trevigen, Gaithersburg, MD); anti-actin polyclonal antibody (Sigma, St. Louis, MO); anti-EGFR and anti-PARP polyclonal antibodies (Upstate Biotechnology, Lake Placid, NY); horseradish peroxidase-conjugated mouse or rabbit secondary antibody (Jackson ImmunoResearch Laboratories, West Grove, PA); etoposide, aphidocolin, and nocodazole (Sigma); WST-1 cell proliferation reagent (Roche, Indianapolis, IN); human recombinant active caspases-3 (BD Pharmingen, San Diego, CA); and DEVD-fmk caspase-3 inhibitor (Calbiochem, San Diego, CA).

BRCC3 cDNA cloning. N-terminal Myc-tagged BRCC3 ORF was amplified by PCR using 100 ng of IMAGE clone (GenBank accession no. BC019075) containing pOTB7 plasmid (ResGen Invitrogen Corp., Huntsville, AL). The forward primer sequence containing *BglII* restriction site (bold), Kozak sequence, translation initiation codon, and the Myc epitope (underlined) was 5'-G**AGATCT**GCCATGGAG CAGAAACTCATCTCTGAAGAGGACCTGATGGAGCA TCGCATCGTGGGG-3', and the reverse primer sequence containing *Mlu1* restriction site (bold) was 5'-G**ACGCGT**C TAGCACCTGTTGCTGTGGAAG-3'. The PCR conditions were as follows: 94˚C for 2 min; denaturation at 94˚C for 30 sec; annealing at 65˚C for 90 sec; extension at 72˚C for 90 sec; and a final extension at 72˚C for 7 min. Twenty-five cycles were performed. The amplified PCR product (1661 bp) was visualized by 1% agarose gel electrophoresis and cloned into the pCR3.1 TA mammalian expression vector (Invitrogen) according to the manufacturer's instructions. BRCC3 cDNA coding sequence (1590 bp) was verified by automated DNA sequencing of both strands using the vector primers (T7 and bovine growth hormone reverse).

Transient and stable cDNA transfections. COS-1 cells were transiently transfected using Lipofectamine 2000 (Invitrogen, Carlsbad, CA) according to the manufacturer's protocol. Briefly, $2x10^6$ cells were seeded into a T-75 tissue culture flask. The following day, cells were transfected with 10 μg of pCR3.1 plasmid containing BRCC3 cDNA Myc-tagged at the N-terminus or pCR3.1 empty vector. At 6 h post-transfection, medium was replaced with DMEM containing 10% FBS and, at 48 h post-transfection, the cells were lysed for Western blotting.

For transient transfection of HEK-293T cells, 60-mm tissue culture dishes were pretreated with 0.1 mg/ml poly-L-Lysine (Sigma) for 8 h at 37˚C. Culture dishes were washed twice with 1X PBS. Approximately $5x10^5$ cells were seeded per dish containing DMEM supplemented with 10% FBS. Twenty-four hours later, the cells were transiently transfected with 2 μg of pCR3.1 (empty vector) or Myc-BRCC3 using 10 μl of Lipofectamine 2000 (Invitrogen) according to the manufacturer's protocol. At 6 h post-transfection, medium was replaced with DMEM containing 10% FBS and, at 48 h post-transfection, cells were washed twice with ice-cold 1X PBS and lysed for Western blotting.

MCF-7 cells were grown in DMEM containing 10% FBS and 25 μg/ml gentamycin, and 90% confluent T-75 tissue culture flasks were subcultured at 1:3 in DMEM containing 10% FBS. After 24 h, cells were transfected with pCR3.1 or Myc-BRCC3 (10 μg/T-75 flask) using 20 μl Lipofectamine 2000. Forty-eight hours after transfection, cells were subcultured at 1:4 and grown in DMEM supplemented with 10% FBS and geneticin (G418, 800 μg/ml) (Invitrogen/Gibco). Selection of transfection-positive cells in G418-containing medium continued for 2 weeks. Approximately 200 G418-resistant colonies were pooled, and pooled stable transfectants were maintained in DMEM supplemented with 10% FBS and G418 (800 μg/ml).

siRNA transfections. MDA-MB 231 cells were seeded in 6-well plates ($1x10^5$ cells/well) or 100-mm dishes ($1.0x10^6$ cells/dish) in complete DMEM medium without antibiotics, and incubated overnight. On the following day, the medium was switched to OPTI-MEM I (Invitrogen/GIBCO) containing 200 nM siRNA (Raf-1, B-Raf, or BRCC3) and Oligofectamine (Raf-1 siRNA or B-Raf siRNA) or Lipofectamine 2000 complex (BRCC3 siRNA) prepared according to the suppliers instructions (Invitrogen/GIBCO). Control cells were treated with a scrambled siRNA (200 nM), Oligofectamine or Lipofectamine

ne, or left untreated. At 4-6 h post-transfection, DMEM containing 10% FBS and antibiotics was added to the medium. After 72 h, cells were lysed in lysis buffer (1% Triton X-100, 0.1% SDS, 0.5% sodium deoxycholate, 10 mM NaCl) containing protease inhibitor cocktail (Roche) and cell lysates were analyzed by Western blotting. The following siRNA duplex sequences were custom made (Invitrogen): B-Raf siRNA (37), sense, 5'-AAG UGG CAU GGU GAU GUG GCA-3'; Raf-1 siRNA (38), sense, 5'-UGU GCG AAA UGG AAU GAG CTT-3'; and scrambled siRNA (37), sense, 5'-AAG UCC AUG GUG ACA GGA GAC-3'. The BRCC3 siRNA duplex sequence (BRCC3 siRNA), BRCC3 pooled siRNA sequences (BRCC3 pl-siRNA), and a control siRNA duplex were obtained commercially (Dharmacon). These duplex sequences were as follows: BRCC3 siRNA, sense, 5'-GUA CUG GGU UUG UUA CAG AUU-3' (Dharmacon, no. D-013830-01); BRCC3 pl-siRNA (Dharmacon, no. M-013830-00-0005); and scrambled (Scr) siRNA (siCONTROL Non-targeting siRNA # 1; Dharmacon, no. D-001210-01-20).

Antisense oligonucleotide treatment. A 20-mer phosphorothioated antisense c-raf-1 oligodeoxyribonucleotide (ISIS 5132) (5'-TCC-CGC-CTG-TGA-CAT-GCA-TT-3') (Raf-1 AS ODN) and a phosphorothioated mismatch antisense oligo (ISIS 10353) (5'-TCC-CGC-GCA-CTT-GAT-GCA-TT-3') (MM ODN) were originally provided by Dr. Brett Monia (ISIS Pharmaceuticals, Carlsbad, CA). (39). All oligos were reconstituted in 1X PBS (1 mg/ml). MDA-MB 231 cells were grown to approximately 70% confluency in T-25 flasks. On day 1, cells were rinsed twice with serum-free medium and treated with 2 ml of serum-free medium containing 26 μl of 1 mg/ml of Raf-1 AS ODN, and 40 μl of Lipofectin per T-25 flask for 6 h (AS ODN final concentration, 2 μM). Control cells were treated with 2 ml of serum-free medium containing 26 μl of 1 mg/ml control mismatch (MM) antisense oligo and 40 μl of Lipofectin per T-25 flask (MM ODN final concentration, 2 μM). The cells were rinsed twice with complete medium containing serum and switched to 2 ml complete medium containing the oligo (as above) without Lipofectin for 18 h. On day 2, day 1 steps were repeated. On day 3, adherent cells were lysed and lysates were used for Western blotting.

Etoposide treatment. Approximately 5x10^5 HEK-293T cells were seeded into 60-mm tissue culture dishes containing DMEM supplemented with 10% FBS. Twenty-four hours later, the cells were transiently transfected with 2 μg of pCR3.1 (empty vector) or Myc-BRCC3 as described above. Twenty-four hours after transfection, the medium was switched to DMEM containing 5% FBS and etoposide (25 μg/ml). Stock solution (30 mg/ml) of etoposide was prepared in DMSO. At various time points, both floating and adherent cells were collected by trypsinization. Approximately 5x10^5 cells were fixed in absolute ethanol, followed by FACS analysis using FACsort (BD Biosciences, San Diego, CA). Remaining cells were lysed for Western blot analysis.

PC-3 cells were seeded into 100-mm tissue culture dishes (1x10^5 per dish) containing DMEM supplemented with 10% FBS and 25 μg/ml gentamycin. On the following day, the medium was switched to DMEM containing 5% FBS and etoposide (40 μg/ml). At various time points, both floating and adherent cells were collected by trypsinization, and lysed in lysis buffer. The cell lysates were analyzed by Western blotting.

Cell synchronization. Logarithmically growing MDA-MD 435 cells were cultured in DMEM supplemented with 10% FBS and treated with 4 μg/ml aphidicolin for 24 h. After 24 h, the cells were washed three times with 1X PBS and incubated in fresh medium for various times. Cells (1x10^6) were fixed in absolute ethanol and cell cycle distribution profiles were examined by FACS analysis. An aliquot of cells at each time point was lysed and proteins analyzed by Western blotting. For synchronization at G2/M phase only, MDA-MB 435 cells and HeLa cells were treated with 100 ng/ml of nocodazole (Sigma) for 16 h. M-phase arrested cells were dislodged by shaking and washed three times with 1X PBS, followed by FACS analysis and Western blotting.

Subcellular fractionation. Cells were fractionated into cytosolic, membrane and nuclear fractions as previously described (40). In brief, approximately 2x10^6 COS-1 cells were seeded in T-75 flasks in DMEM supplemented with 10% FBS. Twenty-four hours later, the cells were transiently transfected with 10 μg of pCR3.1 (empty vector) or Myc-BRCC3. Forty-eight hours after transfection, cells from 4 T-75 flasks were trypsinized and washed with cold PBS. The cell pellet was resuspended (500 μl per T-75 flask) in low-salt homogenization buffer (LS-HB) containing 100 mM HEPES, pH 7.4, 10 mM KCl, 1.5 mM $MgCl_2$, 5 mM EDTA, and 1 mM dithiothreitol and incubated on ice for 20 min. The cells were then homogenized by 100 strokes with a Dounce homogenizer with a tight fitting pestle. The homogenate was centrifuged at 1000 x g for 10 min at 4˚C. The pellet represented the nuclear material. The supernatant was centrifuged at 120,000 x g for 1 h at 4˚C. The resulting supernatant was collected as the cytosolic fraction and the pellet as the membrane fraction. The initial nuclear pellet was washed three times in LS-HB. The nuclear proteins were extracted by resuspending the nuclear pellet (125 μl per flask) in high salt homogenization buffer (i.e. LS-HB containing 750 mM KCl), followed by incubation by rotation at 4˚C for 15 min, and centrifugation at 16,000 x g for 1 h. The supernatant was collected as the nuclear fraction. Cell fractions were resolved by 4-12% Bis-Tris gradient SDS gel electrophoresis (NuPAGE) (Invitrogen) and analyzed by Western blotting.

Northern blot analysis. Expression of BRCC3 mRNA during various phases of the cell cycle was examined in MDA-MB 435 cells by Northern blotting using radiolabeled BRCC3 cDNA as a probe as described previously (41).

Western blot analysis. Cells were washed twice with ice-cold 1X PBS and scraped in NP-40 lysis buffer containing 50 mM Tris-HCl (pH 7.4), 150 mM NaCl, 1% NP-40 (w/v), 10% glycerol (w/v), supplemented with a protease inhibitor pellet and phosphatase inhibitor cocktails I and II (Roche, Indianapolis, IN). The lysates were incubated on ice for 30 min with vortexing for 5 sec every 10 min. Cell lysates were centrifuged for 20 min at 14,000 x g at 4˚C and supernatants

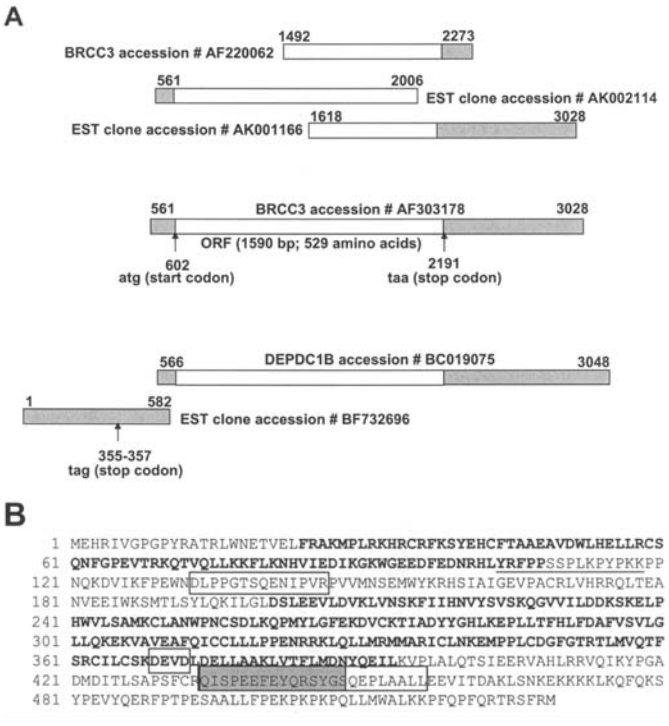

Figure 1. cDNA and predicted amino acid sequences of BRCC3. (A) Schematic maps of the complete BRCC3 cDNA and overlapping ESTs. The open boxes represent the open reading frame (ORF), and gray shaded boxes represent the 5'- and 3'- untranslated regions of the cDNA sequence. (B) The amino acid sequence of BRCC3 indicating conserved domains and putative protein interaction sites. Sequences in bold represent the N-terminal DEP and C-terminal RhoGAP-like conserved domains. The underlined sequence indicates the putative p85 interaction site (P111). The bold and boxed sequence indicates a DEVD caspase-3 cleavage motif. Boxed regions indicate putative DNA-PK (S139 and S448), and/or ATM interaction sites (S448). The shaded and boxed region indicates a putative PDK1 interaction site (E441).

collected. Of the total protein, 25-50 μg was resolved by 10% SDS-PAGE or 4-12% Bis-Tris NuPAGE (Invitrogen), and subsequently transferred to a polyvinylidene difluoride membrane (0.45 μm) (Invitrogen). Western blotting was performed with a desired primary antibody and peroxidase-conjugated secondary antibody, followed by the ECL Plus detection assay (Amersham, Piscataway, NJ).

Flourescence in situ hybridization. To determine the chromosomal location of the human *BRCC3* gene, 4 bacterial artificial chromosome (BAC) clones (RP11-22G5, RP11-946G20, RP11-94L17, and RP11-62I16) with significant sequence homology with the *BRCC3* genomic sequence were selected using the human genome browser at UCSC and were obtained from BACPAC Resources (Oakland, CA) for use as FISH probes. BAC clone DNA was prepared and labeled with biotin-11-dUTP (Roche) using nick translation and hybridized to normal human metaphase spreads as reported previously (42). Biotin-labeled DNA was detected with Fluorescein-Avidin DCS (Vector Labs). Chromosome identification was performed with simultaneous DAPI staining, which produces a Q-banding pattern. Digital images were obtained using a cooled CCD (charge coupled device) camera mounted on a standard fluorescence microscope (Leica). Fluorescein and DAPI images were recorded separately as gray-scale images and then merged using the software package NIH 1.57 and band assignment of the fluorescein signal was performed. For each BAC clone, 15 metaphases were analyzed.

Cell proliferation assay. Approximately 5x10^5 HEK-293T cells were seeded into 60-mm tissue culture dishes with DMEM supplemented with 10% FBS. Twenty-four hours later, the cells were transiently transfected with 2 μg of pCR3.1 (empty vector) or Myc-BRCC3. Six hours after transfection, the cells were trypsinized, and reseeded into a 96-well plate (1x10^4 cells/well, in triplicate) in 100 μl DMEM supplemented with 10% FBS. At 24, 48, and 72 h post-reseeding, 10 μl WST-1 cell proliferation reagent (Roche) was added to the wells and incubation continued for 1 h at 37˚C. Formazan dye absorbance was measured at 450 nm with a Wallac Victor^2 1420 multilabel counter plate reader (Perkin-Elmer, Wellesley, MA).

Results

Identification of BRCC3 cDNA and predicted amino acid sequences. An NCBI BLAST search (http://www.ncbi.nlm.nih.gov) of the human expressed sequence tag (EST) database with the 782-bp BRCC3 cDNA sequence (GenBank accession no. AF220062) revealed the 5'- (GenBank accession no. AK002114 and BF732696) and 3'-overlapping EST clones (GenBank accession no. AK001166). The full-length BRCC3 cDNA (3048 bp) codes for a novel longest ORF comprised of 529 amino acids (aa) (GenBank accession no. AF303178 and BC019075) and contains a characteristic stop codon upstream of the translation initiation site (Fig. 1A). The BRCC3 cDNA coding sequence (1590 bp) was similar to XTP8, human gene 8 transactivated by hepatitis B virus X antigen (GenBank accession no. AF490257). Prosite Scan, a conserved domain database (http://www.expasy.ch/prosite), search revealed an N-terminal DEP (Dishevelled, Egl-1, Pleckstrin) domain (aa 24-108) and a C-terminal Rho-GAP (GTPase activating protein) like domain (aa 201-393). Predicted post-translational modification sites in the ORF are two N-glycosylation sites (aa 18-21 and 255-258), ten casein kinase II phosphorylation sites (aa 45-48, 138-141, 202-205, 274-277, 367-370, 401-404, 402-405, 436-439, 466-469, 480-483), two cAMP-dependent phosphorylation sites (aa 69-72, 157-160), three PKC phosphorylation sites (aa 68-70, 466-468, 526-528), and one tyrosine sulfation site (aa 435-449). A Scansite (http://www.scansite.mit.edu) search for protein-protein interaction motifs predicted putative interactions with p85 (aa 104-118), DNA-protein kinase (aa 133-146 and aa 441-455), ATM kinase (aa 441-455), and PDK1 (aa 434-448). A DEVD caspase-3 cleavage motif was also identified at the C-terminus (aa 369-372) (Fig. 1B).

Chromosomal mapping of BRCC3. Four bacterial artificial chromosome (BAC) clones (RP11-22G5, RP11-946G20, RP11-94L17, and RP11-62I16) containing the BRCC3 genomic sequence were identified through the website (http://www.genome.ucsc.edu) and sequence homology with the BRCC3 cDNA (GenBank accession no. AF303178) was verified via NCBI BLAST search. The BRCC3 gene was mapped to human chromosome 5q12.1 by fluorescence

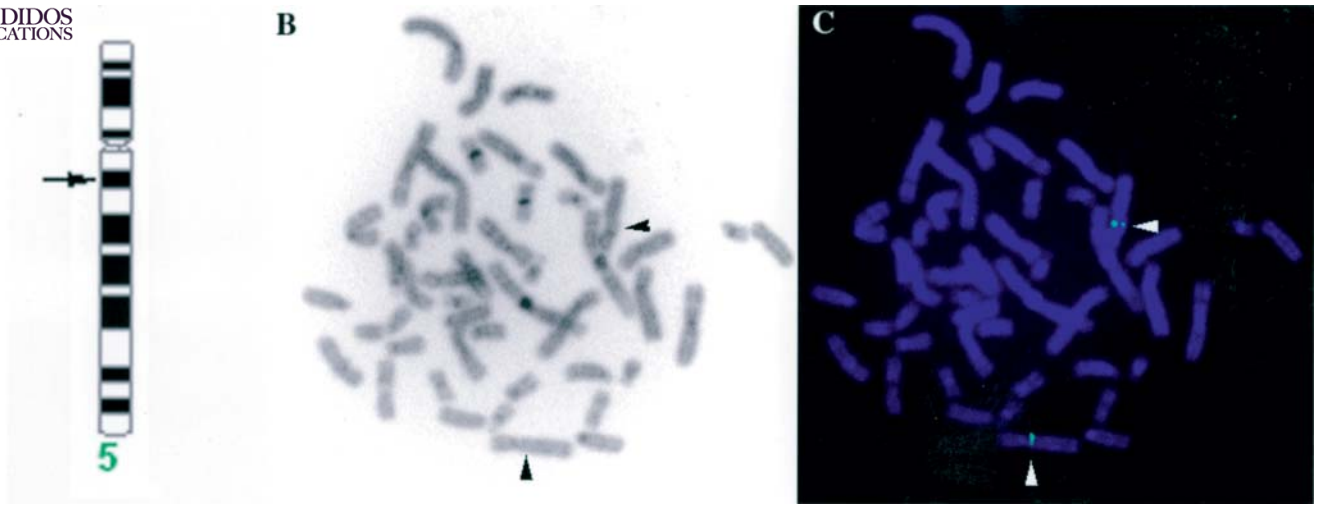

Figure 2. Assignment of BRCC3 to human chromosome 5q12.1. (A) An ideogram of 5q with arrows showing the hybridization site of the four BAC clones on 5q12.1 by FISH. (B) An electronically inverted DAPI image of a representative metaphase spread (inverted DAPI images give a G-band like appearance). Arrow heads point to the location of the RP11-22G5 BAC clone on 5q12.1. (C) The FITC image of that same metaphase spread with arrow heads pointing to the FISH signals.

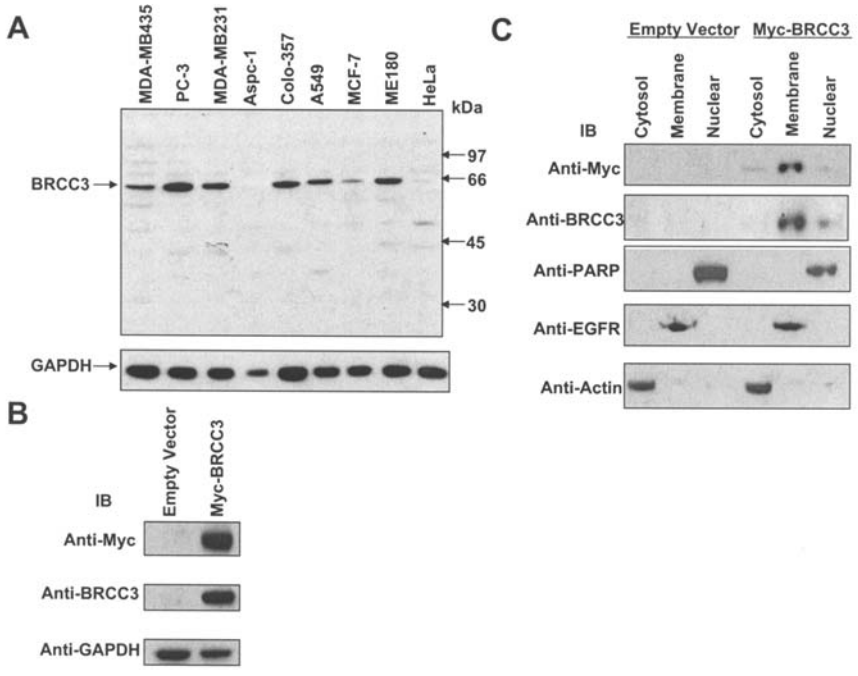

Figure 3. Expression and subcellular localization of BRCC3. (A) Expression of endogenous BRCC3 protein in human cancer cell lines. Fifty micrograms of protein from whole cell lysate was analyzed by 10% SDS-PAGE and Western blotting using anti-BRCC3 antibody. The blot was reprobed with anti-GAPDH antibody. MDA-MB 435, breast ductal carcinoma; PC-3, prostate carcinoma; MDA-MB 231, breast carcinoma; Aspc-1, pancreatic adenocarcinoma; Colo-357, pancreatic carcinoma; A549, lung carcinoma; MCF-7, breast adenocarcinoma; ME-180, cervical carcinoma; HeLa, cervical carcinoma. (B) Expression of BRCC3 cDNA in COS-1 cells. COS-1 cells ($2x10^6$) were transiently transfected with Myc-BRCC3 cDNA or pCR3.1 empty vector. Whole cell lysate (25 μg of protein) was analyzed by 4-12% Bis-Tris NuPAGE and Western blotting. The same blot was sequentially probed with anti-Myc, anti-BRCC3, and anti-GAPDH antibodies. IB, immunoblotting. (C) Subcellular localization of BRCC3. The cytosolic, membrane, and nuclear fractions (25 μg of protein) from COS-1 cells transiently transfected with Myc-BRCC3 or pCR3.1 empty vector were analyzed by 4-12% Bis-Tris NuPAGE and Western blot analysis. The same blot was sequentially probed with anti-Myc, anti-BRCC3, anti-PARP, anti-EGFR, and anti-actin antibodies.

in situ hybridization (FISH). For each BAC clone, a specific hybridization signal was detected in all 15 metaphases analyzed on both chromatids of chromosome 5 localized to 5q12.1. No other hybridization sites were observed. Fig. 2 shows the FISH mapping data with a representative metaphase image showing the hybridization of BAC RP11-22G5 to chromosome 5q12.1.

Expression and subcellular localization of BRCC3. A rabbit polyclonal anti-peptide antibody was custom generated against the C-terminus portion of BRCC3 (aa 517-529). The anti-BRCC3 antibody recognized a 60-kDa protein in various human cancer cell lines tested (Fig. 3A). The protein was not detectable with the pre-immune serum (data not shown). The BRCC3 ORF tagged at the N-terminus with Myc epitope was

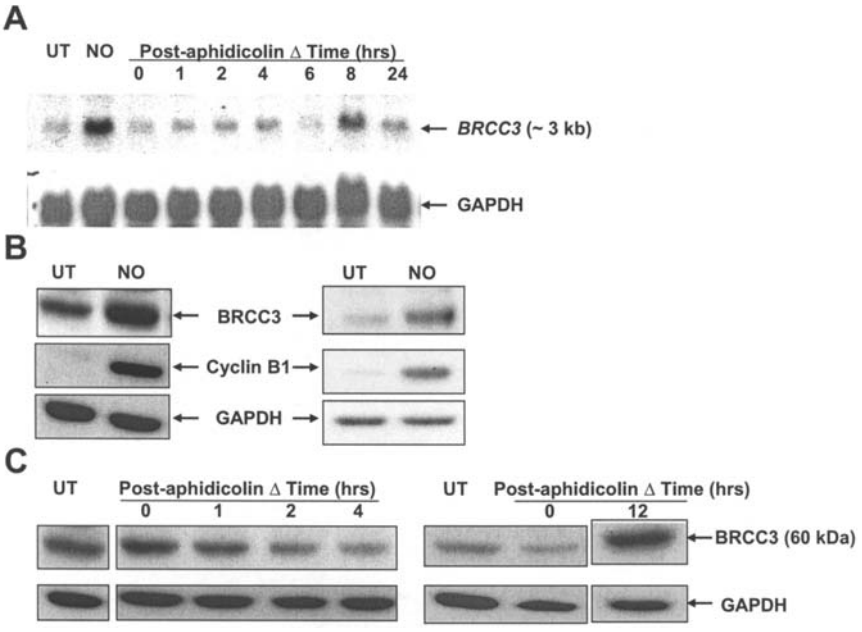

Figure 4. Enhanced levels of BRCC3 mRNA and protein expression during G2/M phase. (A) Expression of *BRCC3* mRNA during cell cycle in MDA-MB 435 cells. Total RNA was isolated from MDA-MB 435 cells treated with nocodazole (NO, 100 ng/ml, 16 h) or aphidicolin (4 μg/ml, 24 h) and incubated in fresh medium without aphidicolin for indicated times. Expression of BRCC3 mRNA in cells enriched in G1, S, or G2/M phase was analyzed by Northern blotting using radiolabeled BRCC3 cDNA (GenBank accession no. AF220062) as probe. The blot was reprobed with radiolabeled GAPDH cDNA and signals were quantified using Image-Quant software. The fold change in *BRCC3* mRNA expression relative to untreated cells (UT) was calculated after normalizing the expression against GAPDH signal in the corresponding lane. 0 h post-aphidicolin, G1; 2 h post-aphidicolin, S; NO-treated and 8 h post-aphidicolin, G2/M. (B) Effect of nocodazole on BRCC3 protein expression. MDA-MB 435 cells (left panel) or HeLa cells (right panel) were enriched in G2/M phase by treatment with nocodozole (100 ng/ml, 16 h). Cell lysates were analyzed by 10% SDS-PAGE and Western blotting. The blot was sequentially probed with antibodies against BRCC3, Cyclin B1 (a marker for G2/M phase), and GAPDH. The BRCC3 protein expression was normalized against GAPDH expression in the corresponding lane. The fold change in normalized BRCC3 expression relative to untreated cells (UT) was calculated. (C) Expression of BRCC3 protein during cell cycle in MDA-MB 435 cells. Whole cell lysates were isolated from MDA-MB 435 cells at indicated times post-aphidocolin treatment (4 μg/ml, 24 h), and resolved by 10% SDS-PAGE, followed by Western blot analysis. The right and left panels shown are two independent experiments. The blot was probed with anti-BRCC3 antibody and reprobed with anti-GAPDH antibody. The signals were quantified as in B. 0 h post-aphidicolin, G1; 2 h post-aphidicolin, S; 12 h post-aphidicolin, G2/M.

cloned into pCR3.1 mammalian expression vector (Myc-BRCC3). In COS-1 cells transiently transfected with Myc-BRCC3, BRCC3 expression (60 kDa) was detected with both the anti-BRCC3 polyclonal antibody and anti-Myc monoclonal antibody (Fig. 3B). The BRCC3 ORF contains an N-terminal DEP domain, and DEP domains in other proteins, including Dishevelled-1 (Dvl-1) have been implicated in membrane translocation following signal stimulation (43). Subcellular localization of BRCC3 protein was investigated in the transiently transfected COS-1 cells. Western blot analysis of the cytosolic, membrane, and nuclear fractions revealed that the exogenous BRCC3 was predominantly localized to the membrane in COS-1 transfectants (Fig. 3C).

Increased expression of BRCC3 at G2/M phase. We next examined BRCC3 mRNA and protein expression during the cell cycle. MDA-MB 435 breast cancer cells were enriched in G2/M phase of the cell cycle by treatment with nocodazole (NO) [untreated (UT): G2/M, ~14%; NO-treated: G2/M, ~76%; n=2]. In addition, these cells were enriched in G1 phase by treatment with aphidicolin (UT: G1, ~41%; S, ~46%; G2/M, ~14%; aphidicolin-treated: G1, ~57%; S, ~38%; G2/M, ~5%; n=2), followed by incubation in aphidicolin-free medium for various times. At 2 h post-aphidicolin treatment, cells were found predominantly in S phase (G1, 0%; S, 89%; G2/M, 11%). At 8 and 12 h post-aphidicolin release, cells were enriched in G2/M phase (8 h post-aphidicolin: G1, 3%; S, 17%; G2/M, 80%; 12 h post-aphidicolin: G1, 24%; S, 24%; G2/M, 52%). BRCC3 transcript level (~3.0 kb) was found to be elevated following NO treatment (5.0-fold versus UT), and at 8 h post-aphidicolin release in MDA-MB 435 cells (4.0-fold versus UT) (Fig. 4A). BRCC3 protein level was increased in NO-treated cells (3.4-fold versus UT) (Fig. 4B, left panel), and at 12 h post-aphidocolin treatment of MDA-MB 435 cells (4.9-fold versus UT) (Fig. 4C). In addition, NO treatment of HeLa cells led to increased G2/M population (UT: G2/M, 13%; NO-treated: G2/M, 90%) and an increase in BRCC3 protein expression (4.0-fold versus UT) (Fig. 4B, right panel). These data demonstrate that BRCC3 mRNA and protein levels are relatively high during G2/M phase of the cell cycle.

Effects of inhibition of Raf proteins on BRCC3 expression. In a previous study, we observed that BRCC3 mRNA expression was decreased in MDA-MB 231 breast cancer cells treated with Raf-1 antisense oligonucleotide (Raf-1 AS ODN) (Gokhale *et al*, unpublished data). Here we investigated whether BRCC3 protein level is modulated by downregulation of Raf-1 or B-Raf. MDA-MB 231 cells were treated with siRNA against Raf-1 (Fig. 5A) or B-Raf (Fig. 5B), or with c-raf-1 antisense oligonucleotide (Fig. 5C). In the siRNA experiments, expression of Raf-1 or B-Raf in untreated and

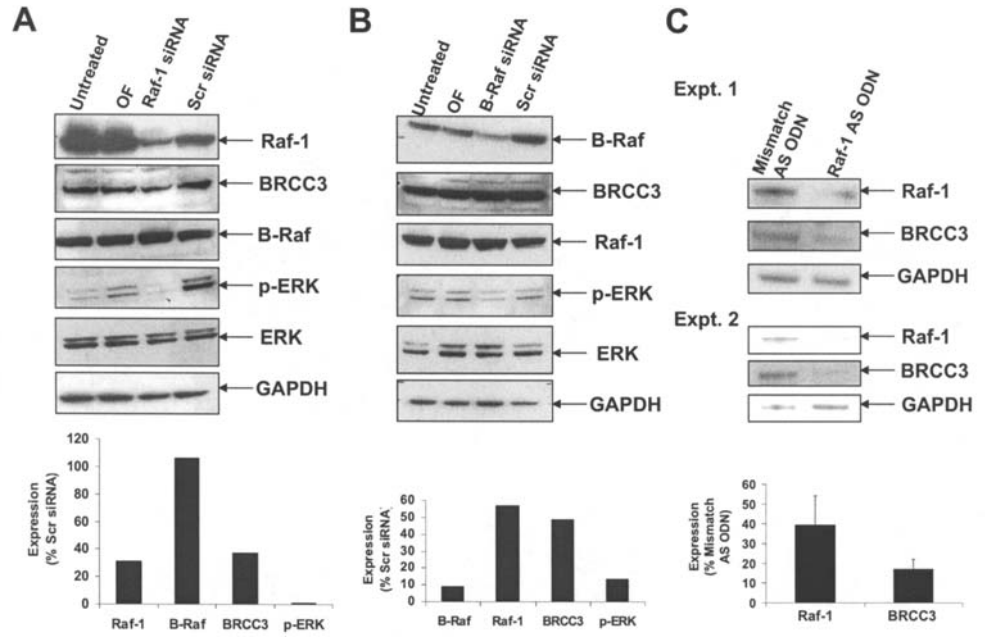

Figure 5. Effects of inhibition of Raf-1 or B-Raf on BRCC3 and phospho-ERK expression in MDA-MB 231 cells. (A) Effects of siRNA inhibition of Raf-1. MDA-MB 231 cells were transfected with Raf-1 siRNA (200 nM) using Oligofectamine. Control cells were treated with a scrambled control siRNA (Scr siRNA, 200 nM), Oligofectamine (OF), or left untreated. Cell lysates were analyzed by 4-12% bis-Tris NuPAGE and immunoblotting with anti-Raf-1 antibody. The same blot was sequentially reprobed with anti-BRCC3, anti-B-Raf, anti-p-ERK, anti-ERK, and anti-GAPDH antibodies (top panel). The signals were quantified using ImageQuant software and normalized against GAPDH signals in the corresponding lanes. Expression relative to Scr siRNA control was plotted (bottom panel). (B) Effects of siRNA inhibition of B-Raf. MDA-MB 231 cells were treated with 200 nM of B-Raf siRNA as in A. Control cells were treated with a control siRNA (Scr siRNA, 200 nM), Oligofectamine (OF), or left untreated. Cell lysates were analysed by immunoblotting with anti-B-Raf antibody. The same blot was sequentially reprobed with anti-BRCC3, anti-Raf-1, anti-p-ERK, anti-ERK, and anti-GAPDH antibodies (top panel). The signals were quantified using ImageQuant software and normalized against GAPDH signals in the corresponding lanes. Expression relative to Scr siRNA control was plotted (bottom panel). (C) Antisense c-*raf-1* oligonucleotide treatment inhibits BRCC3 protein expression. MDA-MB 231 cells were treated with 2 μM of mismatch antisense oligonucleotide (AS ODN) or antisense *raf-1* oligonucleotide (Raf-1 AS ODN) as described in Materials and methods. Top and middle panels, 4-12% Bis-Tris NuPAGE and Western blot analysis was performed using whole cell lysates. The blot was sequentially probed with anti-Raf-1, anti-BRCC3, and anti-GAPDH antibodies. Bottom panel, quantification (mean ± S.D.) of BRCC3 and Raf-1 protein expression shown in top and middle panels.

oligofectamine (OF) control groups was found to be different as compared to the scrambled siRNA control group (Fig. 5A and B). All data have been quantified relative to the scrambled group. Treatment of MDA-MB 231 cells with Raf-1 siRNA caused significant inhibition of Raf-1, BRCC3, and p-ERK [Raf-1 siRNA (200 nM), inhibition % scrambled siRNA: Raf-1, 69%; BRCC3, 63%; p-ERK, 99%], and no change in B-Raf expression (Fig. 5A). Treatment of MDA-MB 231 cells with B-Raf siRNA led to a high inhibition of B-Raf and p-ERK, and relatively less inhibition of Raf-1 and BRCC3 [B-Raf siRNA (200 nM), inhibition, % scrambled siRNA: B-Raf, 91%; p-ERK, 87%; Raf-1, 43%; BRCC3, 51%] (Fig. 5B). BRCC3 expression was also significantly inhibited in MDA-MB 231 cells treated with c-raf-1 antisense oligonucleotide (2 μM) (% mismatch antisense oligo: Raf-1, 61%; BRCC3, 83%) (Fig. 5C). These data suggest that BRCC3 expression is regulated by changes in the level of Raf, predominantly Raf-1 in MDA-MB 231 cells.

Effect of modulation of BRCC3 on phospho-ERK expression. Increased expression of p-ERK is a hallmark of cell survival and proliferation. To investigate a potential role of BRCC3 in oncogenesis, we asked whether modulation of BRCC3 expression results in a concomitant modification of the constitutive level of p-ERK. Myc epitope-tagged BRCC3 cDNA was transiently transfected into COS-1 or HEK-293T cells. Following transfection, cells were grown in serum-containing medium for 48 h and the cell lysates were examined by Western blotting (Fig. 6A). We observed an approximate 2- to 5-fold increase in p-ERK in BRCC3 transfectants as compared to empty vector transfectants in both cell types (n=3). The expression of endogenous Raf-1 was not changed in HEK-293T cells transfected with Myc-BRCC3 as compared with empty vector transfectants (data not shown). Similar observations were made in MCF-7 cells stably transfected with Myc-BRCC3 (Fig. 6B). Cross-talk between MAPK and PI-3 kinase signaling pathways is a likely event in certain cell types. There was no change in constitutive expression of phospho-AKT, an important effector of PI-3 kinase, in BRCC3 cDNA transfected COS-1 cells (data not shown). We next determined the effect of inhibition of endogenous BRCC3 on p-ERK. Treatment of MDA-MB 231 cells with BRCC3 siRNA or BRCC3 pooled siRNA (pl-siRNA) caused a significant decrease of BRCC3 and a moderate reduction in p-ERK [BRCC3 siRNA/pl-siRNA (200 nM), inhibition, % scrambled siRNA: BRCC3, 82%; p-ERK, 55%] (Fig. 6C).

Correlation between BRCC3 expression, cell survival and proliferation. As a step towards understanding the biological function of BRCC3, we determined the effect of BRCC3 expression on cell survival and cell proliferation. Transiently transfected HEK-293T cells were treated with etoposide, and

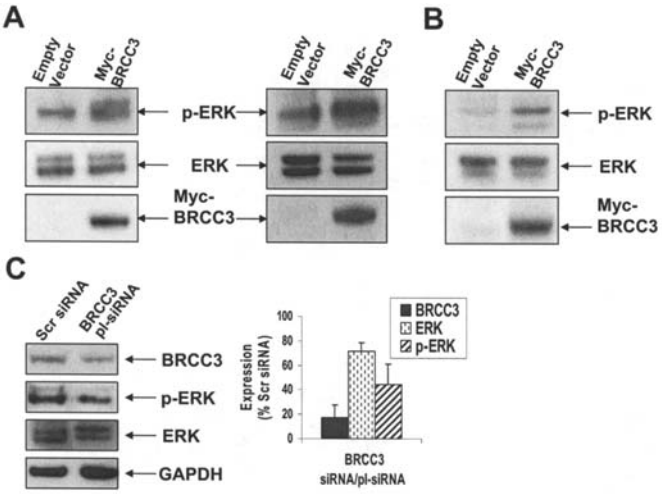

Figure 6. Effect of modulation of BRCC3 on phospho-ERK expression. (A) COS-1 cells (left panel) or HEK-293T cells (right panel) ($5x10^5$) were transiently transfected with either Myc-BRCC3 or empty vector (2 μg). After 48 h in serum-containing medium (10% FBS), whole cell lysates were collected and 30 μg of protein was analyzed by 4-12% Bis-Tris NuPAGE and Western blotting. The blot was sequentially probed with anti-phospho-ERK (p-ERK), anti-ERK and anti-Myc antibodies. The fold increase in p-ERK/total ERK expression in BRCC3 transfectants versus empty vector transfectants was determined by densitometry (ImageQuant software). The data shown are representative of three independent experiments. (B) MCF-7 cells were stably transfected with Myc-BRCC3 or empty vector as described in Materials and methods. Cell lysates were analyzed by Western blotting as in A. (C) MDA-MB 231 cells were transfected with 200 nM of BRCC3 siRNA, BRCC3 pooled siRNA (pl-siRNA), or scrambled siRNA (Scr siRNA). After 72 h in serum-containing medium (10% FBS), whole cell lysates were analyzed by Western blotting, and the blots were sequentially probed with anti-BRCC3, anti-p-ERK, anti-ERK, and anti-GAPDH antibodies (left panel). The signals were quantified using ImageQuant software and normalized against GAPDH signals in the corresponding lanes. Expression relative to Scr siRNA control was plotted (right panel).

the number of sub-G1 cells, indicative of cell death, was quantified by flow cytometry. At 12 h following etoposide treatment, an approximate 2.0-fold increase in sub-G1 cells was observed in control vector transfected cells relative to untreated cells. In contrast, no change in number of sub-G1 cells was observed up to 16 h in etoposide-treated Myc-BRCC3 transfectants. However, vector and Myc-BRCC3 transfectants showed a comparable increase in sub-G1 population by 24 h (~2.5-fold). Exogenous expression of BRCC3 seems to delay etoposide-induced cell death in HEK-293T cells (Fig. 7A, left panel). No apparent change in expression of Myc-BRCC3 (~60 kDa) was observed during the course of etoposide treatment in these cells (Fig. 7A, right panel).

Previous studies have demonstrated that several survival molecules are subject to caspase-dependent cleavage and degradation in response to apoptotic agents, including etoposide, 'turning-off' the interference due to survival pathways (44). To further characterize BRCC3 as a pro-survival signal, we examined the effect of purified, active caspase-3 on BRCC3 *in vitro*. Whole cell lysates from HEK-293T cells transiently transfected with Myc-BRCC3 were pre-incubated with or without DEVD-*fmk*, a caspase-3 specific inhibitor, followed by addition of active caspase-3. By Western blot analysis, a decreased level of BRCC3 (~60 kDa) was evident within 1 h following caspase-3 treatment, whereas no change in BRCC3 expression was observed in cell lysates pre-incubated with DEVD-*fmk* (Fig. 7B). Treatment of the lysates from MCF-7 cells stably transfected with Myc-BRCC3 with purified active caspase-3 also resulted in a decreased level of BRCC3 (~60 kDa) (Fig. 7C). Human PC-3 prostate cancer cells express a moderate level of BRCC3 protein (~60 kDa). As shown in Fig. 7D, etoposide treatment of PC-3 cells was found to cause significant degradation of endogenous BRCC3 within 24 h.

We used the WST-1 assay to examine the effect of transient expression of BRCC3 on cell viability and proliferation in HEK-293T cells. An approximate 30% increase in cell proliferation was seen in Myc-BRCC3 expressing HEK-293T cells at 72 h as compared to the empty vector transfectants (Fig. 7E). Together these results demonstrate a correlation between BRCC3 expression and cell survival and proliferation, and suggest BRCC3 as a potential target of a caspase(s).

Discussion

This study is the first report on BRCC3. We have demonstrated that BRCC3 is a novel cell cycle-regulated molecule. The mechanism of transcriptional/translational upregulation of BRCC3 at G2/M phase is currently not known. A sequence homology search of the chromosome 5 genomic DNA revealed several CCAAT-boxes and E-boxes (CANNTG) within a putative BRCC3 promoter region (3000 bp upstream of the 5'-end of the BRCC3 mRNA) (MatInspector 2.2, TransFac 4.0 matrices: http://transfac.gbf.de). The CCAAT boxes are potential binding sites of transcription factor NF-Y, whereas E-boxes have been shown to bind to upstream stimulatory factors (USFs). By analogy to cyclin B, where the peak mRNA expression at G2/M is linked to cell cycle-dependent usage of transcriptional enhancer motifs within the promoter (GGCT repeats, CCAAT-boxes, E-boxes) (45,46), BRCC3 transcription may be regulated via CCAAT/E-box motifs in a cell cycle-dependent manner. In addition, cell cycle-dependent elements (CDE) (5'-GGCGC-3') and cell cycle gene homology regions (CHR) (5'-TTTGAA-3') in the cyclin B promoter have been shown to repress cyclin B transcription in resting and G1 cells (47,48). Deletion analysis of the BRCC3 promoter will be necessary to establish a basis of transcriptional upregulation of BRCC3 during cell cycle. Raf-1 has been shown to be activated during mitosis (49,50). It is not known whether BRCC3 expression during G2/M is dependent on mitotic Raf-1 kinase. Furthermore, alterations in the BRCC3 mRNA and/or protein stability during the cell cycle cannot be ruled out at this time.

Upregulation of BRCC3 during G2/M phase may have important functional implications. As mentioned earlier, the BRCC3 open reading frame contains putative interaction sites for DNA protein kinase (DNA-PK) and ATM. Both enzymes have been shown to play a key role in DNA damage response pathways associated with control of cell cycle progression (cell cycle checkpoints, including G2/M checkpoint), chromatin restructuring and DNA repair (51-54). It is also known that interaction of these proteins with specific protein partners is essential to their activation and control of checkpoints (54-56). Further studies will investigate a possible interaction between BRCC3 and ATM/DNA-PK and the effect of loss of BRCC3 on damage-induced G2/M checkpoint.

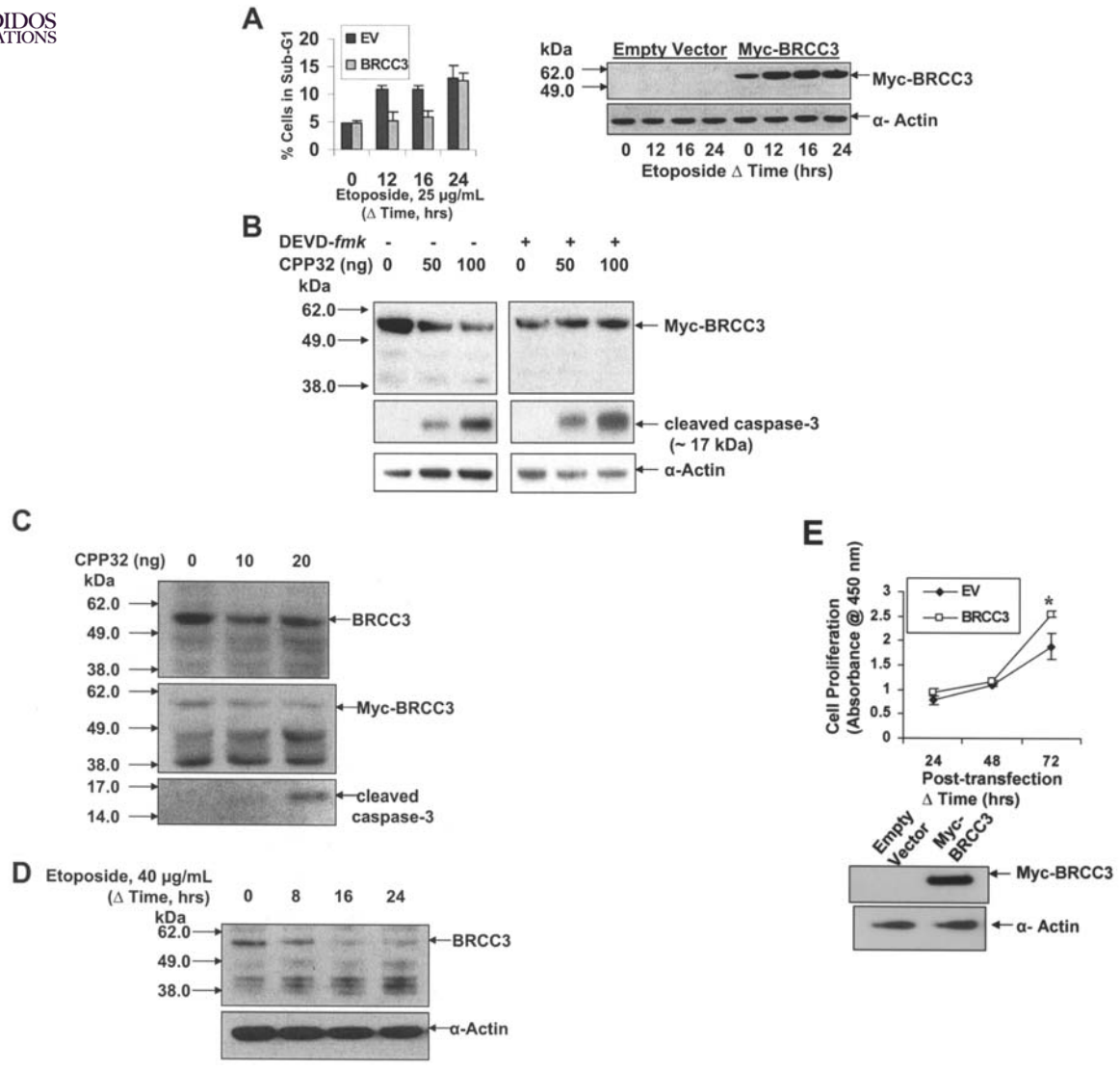

Figure 7. Effects of BRCC3 expression on cell survival and cell proliferation. (A) Effect of BRCC3 on cell survival. HEK-293T cells were transiently transfected with Myc-BRCC3 (gray) or empty vector (black). Twenty-four hours after transfection, cells were treated with etoposide, and floating and adherent cells were collected at indicated time points. Cells were fixed in ethanol and no. of cells in sub-G1 phase was quantified by FACS method. Data shown are mean ± S.D. from two independent experiments (right panel). Expression of Myc-BRCC3 at various times following etoposide treatment was verified by Western blotting using anti-Myc antibody and the blot was reprobed with anti-α-actin antibody (left panel). EV, empty vector. (B) *In vitro* effect of caspase-3 on transiently transfected BRCC3 in HEK-293T cells. HEK-293T cells were transiently transfected with Myc-BRCC3. Forty-eight hours post-transfection, cell lysates (50 μg) were pre-incubated with 100 μM DEVD-*fmk* for 1 h on ice, followed by addition of an indicated amount of purified active caspase-3 (CPP32). Incubation continued for 1 h at 37˚C. Cell lysates were analyzed by 4-12% Bis-Tris NuPAGE and Western blotting. The same blot was sequentially probed with anti-Myc, anti-cleaved/active caspase-3 and anti-actin antibodies. Representative data from one of the two independent experiments are shown. (C) *In vitro* effect of caspase-3 on BRCC3 in stably transfected MCF-7 cells. MCF-7 cells were stably transfected with Myc-BRCC3 or vector as explained in Materials and methods. Cell lysates (50 μg) were incubated with indicated amounts of purified active caspase-3 (CPP32) for 1 h at 37˚C and analyzed by 4-12% Bis-Tris NuPAGE and Western blotting. The same blot was sequentially probed with anti-BRCC3, anti-Myc and anti-cleaved/active caspase-3 antibodies. (D) Effect of etoposide on endogenous BRCC3. PC-3 cells were treated with etoposide for indicated times. Whole cell lysates (50 μg) were resolved by 4-12% Bis-Tris NuPAGE and analyzed by Western blotting with anti-BRCC3 antibody. The blot was reprobed with anti-actin antibody. (E) Effect of BRCC3 on cell proliferation. HEK-293T cells ($5x10^5$) were transiently transfected with 2 μg of Myc-BRCC3 (□) or empty vector (◇). Six hours after transfection, cells were reseeded in triplicate ($1x10^4$ per well) in a 96-well plate containing medium supplemented with 10% FBS. Cell proliferation was assayed at indicated times by WST-1 reduction as described in the Materials and methods [*empty vector (EV) vs. BRCC3, p=0.01] (top panel). Expression of Myc-BRCC3 at 72 h post-reseeding was verified by 4-12% Bis-Tris NuPAGE and Western blotting with anti-Myc antibody. The blot was reprobed with anti-actin antibody (bottom panel).

The mechanism of regulation of BRCC3 expression by Raf-1 is unknown. Regulation of BRCC3 mRNA and protein levels by Raf-1 expression provides several points from which transcription and translation of BRCC3 may be controlled. Increase in BRCC3 expression correlates with enhanced p-ERK, cell survival and cell proliferation. The Raf>MEK>ERK pathway is a known inducer of oncogene expression, thus a positive regulatory loop is possible. Our data show modulation of pERK via BRCC3 expression. These observations may have significant implications. While Raf-1 is not the only activator of ERK, p-ERK expression is an important prognostic indicator of diverse disease types. Future investigations are necessary to delineate the mechanism(s) linking BRCC3 with p-ERK and associated biological responses.

Acknowledgements

This study was funded by National Institutes of Health grants CA68322 and CA74175, and by NeoPharm, Inc.

References

1. Juliano RL, Reddig P, Alahari S, Edin M, Howe A and Aplin A: Integrin regulation of cell signalling and motility. Biochem Soc Trans 32: 443-446, 2004.
2. O'Neill EE, Matallanas D and Kolch W: Mammalian sterile 20-like kinases in tumor suppression: an emerging pathway. Cancer Res 65: 5485-5487, 2005.
3. Kasid U and Suy S: Stress-responsive signal transduction: Emerging concepts and biological significance. In: Apoptosis Genes. Potten CS, Booth C, and Wilson J (eds). Kluwer Academic Publishers, pp85-118, 1998.
4. O'Neill E and Kolch W: Conferring specificity on the ubiquitous Raf/MEK signaling pathway. Br J Cancer 90: 283-288, 2004.
5. von Gise A, Lorenz P, Wellbrock C, Hemmings B, Berberich-Siebelt F, Rapp UR and Troppmair J: Apoptosis suppression by Raf-1 and MEK1 requires MEK and phosphatidylinositol 3-kinase-dependent signals. Mol Cell Biol 21: 2324-2336, 2001.
6. Wan PT, Garnett MJ, Roe SM, Lee S, Niculescu-Duvaz D, Good VM, Jones CM, Marshall CJ, Springer CJ, Barford D, Marais R and Cancer Genome Project: Mechanism of activation of the RAF-ERK signaling pathway by oncogenic mutations of B-RAF. Cell 116: 855-867, 2004.
7. Kasid U, Suy S, Dent P, Ray S, Whiteside TL and Sturgill TW: Activation of Raf by ionizing radiation. Nature 382: 813-816, 1996.
8. Vanderkuur JA, Butch ER, Waters SB, Pessin JE, Guan KL and Carter-Su C: Signaling molecules involved in coupling growth hormone receptor to mitogen-activated protein kinase activation. Endocrinology 138: 4301-4307, 1997.
9. Edin M and Juliano RL: Raf-1 serine 338 phosphorylation plays a key role in adhesion-dependent activation of extracellular signal-regulated kinase by epidermal growth factor. Mol Cell Biol 25: 4466-4475, 2005.
10. Dougherty MK, Muller J, Ritt DA, Zhou M, Zhou XZ, Copeland TD, Conrads TP, Veenstra TD, Lu KP and Morrison DK: Regulation of Raf-1 by direct feedback phosphorylation. Mol Cell 17: 215-224, 2005.
11. York RD, Yao H, Dillon T, Ellig CL, Eckert SP, McCleskey EW and Stork PJ: Rap 1 mediates sustained MAP kinase activation induced by nerve growth factor. Nature 392: 622-626, 1998.
12. Bernal-Mizrachi E, Wen W, Srinivasan S, Klenk A, Cohen D and Permutt MA: Activation of ELK-1 and Ets transcription factor by glucose and EGF treatment of insulinoma cells. Am J Physiol Endocrinol Metab 281: 1286-1299, 2001.
13. Ouwens DM, de Ruiter ND, van der Zon GC, Carter AP, Schouten J, van der Burgt C, Kooistra K, Bos JL, Maassen JA and van Dam H: Growth factors can activate ATF2 via a two-step mechanism: phosphorylation of Thr71 through the Ras-MEK-ERK pathway and of Thr69 through RalGDS-Src-p38. EMBO J 21: 3782-3793, 2002.
14. Patel S, Wang FH, Whiteside TL and Kasid U: Constitutive modulation of Raf-1 protein kinase is associated with differential gene expression of several known and unknown genes. Mol Med 3: 674-685, 1997.
15. Schulze A, Lehmann K, Jefferies HB, McMahon M and Downward J: Analysis of the transcriptional program induced by Raf in epithelial cells. Genes Dev 15: 981-994, 2001.
16. Schulze A, Nicke B, Warne PH, Tomlinson S and Downward J: The transcriptional response of Raf activation is almost completely dependent on mitogen-activated protein kinase kinase activity and shows a major autocrine component. Mol Cell Biol 15: 3450-3463, 2004.
17. Chen J, Fujii K, Zhang L, Roberts T and Fu H: Raf-1 promotes cell survival by antagonizing apoptosis signal-regulating kinase 1 through a MEK-ERK independent mechanism. Proc Natl Acad Sci USA 98: 7783-7788, 2001.
18. O'Neill E, Rushworth L, Baccarini M and Kolch W: Role of the kinase MST2 in suppression of apoptosis by the proto-oncogene product Raf-1. Science 306: 2267-2270, 2004.
19. Ehrenreiter K, Piazzolla D, Velamoor V, Sobczak I, Small JV, Takeda J, Leung T and Baccarini M: Raf-1 regulates Rho signaling and cell migration. J Cell Biol 168: 955-964, 2005.
20. Dhillon AS, Meikle S, Peyssonnaux C, Grindlay J, Kaiser C, Steen H, Shaw PE, Mischak H, Eychene A and Kolch W: A Raf-1 mutant that dissociates MEK/Extracellular signal-regulated kinase activation from malignant transformation and differentiation but not proliferation. Mol Cell Biol 23: 1983-1993, 2003.
21. Kasid U and Dritschilo A: RAF antisense oligonucleotide as a tumor radiosensitizer. Oncogene 22: 5876-5884, 2003.
22. Zhang C, Pei J, Kumar D, Sakabe I, Boudreau H, Gokhale PC and Kasid UN: Antisense oligonucleotides: Target validation and development of systemically-delivered therapeutic nanoparticles. In: Methods in Molecular Biology. Walker JM (ed). Vol 361. Target Discovery and Validation Reviews and Protocols: Emerging Molecular Targets and Treatment Options. Sioud M (ed). Vol II. Humana Press, Totowa, New Jersey, pp163-185, 2006.
23. Gleave ME and Monia BP: Antisense therapy for cancer. Nat Rev Cancer 5: 468-479, 2005.
24. Gokhale PC, Zhang C, Newsome JT, Pei J, Ahmad I, Rahman A, Dritschilo A and Kasid UN: Pharmacokinetics, toxicity, and efficacy of ends-modified raf antisense oligodeoxyribonucleotide encapsulated in a novel cationic liposome (LErafAON). Clin Cancer Res 8: 3611-3621, 2002.
25. Pal A, Ahmad A, Khan S, Sakabe I, Zhang C, Kasid UN and Ahmad I: Systemic delivery of RafsiRNA using cationic cardiolipin liposome silences Raf-1 expression and inhibits tumor growth in xenograft model of human prostate cancer. Int J Oncol 26: 1087-1091, 2005.
26. Wilhelm SM, Carter C, Tang L, Wilkie D, McNabola A, Rong H, Chen C, Zhang X, Vincent P, McHugh M, Cao Y, Shujath J, Gawlak S, Eveleigh D, Rowley B, Liu L, Adnane L, Lynch M, Auclair D, Taylor I, Gedrich R, Voznesensky A, Riedl B, Post LE, Bollag G and Trail PA: BAY 43-9006 exhibits broad spectrum oral anti-tumor activity and targets the Raf/MEK/ERK pathway and receptor tyrosine kinases involved in tumor progression and angiogenesis. Cancer Res 64: 7099-7109, 2004.
27. Rudin CM, Holmlund J, Fleming GF, Mani S, Stadler WM, Schumm P, Monia BP, Johnston JF, Geary R, Yu RZ, Kwoh TJ, Dorr FA and Ratain MJ: Phase I Trial of ISIS 5132, an antisense oligonucleotide inhibitor of c-raf-1, administered by 24-hour weekly infusion to patients with advanced cancer. Clin Cancer Res 7: 1214-1220, 2001.
28. Sridhar SS, Hedley D and Siu LL: Raf kinase as a target for anticancer therapeutics. Mol Cancer Ther 4: 677-685, 2005.
29. Rudin CM, Marshall JL, Huang CH, Kindler HL, Zhang C, Kumar D, Gokhale PC, Steinberg J, Wanaski S, Kasid UN and Ratain MJ: Delivery of a liposomal c-raf-1 antisenseoligonucleotide by weekly bolus dosing in patients with advanced solid tumors: a phase I study. Clin Cancer Res 10: 7244-7251, 2004.
30. Dritschilo A, Huang CH, Rudin CM, Marshall J, Collins B, Dul JL, Zhang C, Kumar D, Gokhale PC, Ahmad A, Ahmad I, Sherman JW and Kasid UN: Phase I study of liposome encapsulated c-*raf* antisense oligodeoxyribonucleotide (LErafAON) infusion in combination with radiation therapy in patients with advanced malignancies. Clin Cancer Res 12: 1251-1259, 2006.
31. Staehler M, Rohrmann K, Haseke N, Stief CG and Siebels M: Targeted agents for the treatment of advanced renal cell carcinoma. Curr Drug Targets 6: 835-846, 2005.
32. Kupsch P, Henning BF, Passarge K, Richly H, Wiesemann K, Hilger RA, Scheulen ME, Christensen O, Brendel E, Schwartz B, Hofstra E, Voigtmann R, Seeber S and Strumberg D: Results of a phase I trial of sorafenib (BAY 43-9006) in combination with oxaliplatin in patients with refractory solid tumors, including colorectal cancer. Clin Colorectal Cancer 5: 188-196, 2005.
33. Clark JW, Eder JP, Ryan D, Lathia C and Lenz HJ: Safety and pharmacokinetics of the dual action Raf kinase and vascular endothelial growth factor receptor inhibitor, BAY 43-9006, in patients with advanced, refractory solid tumors. Clin Cancer Res 11: 5472-5480, 2005.
34. Benn J and Schneider RJ: Hepatitis B virus HBx protein activates Ras-GTP complex formation and establishes a Ras, Raf, MAP kinase signaling cascade. Proc Natl Acad Sci USA 91: 10350-10354, 1994.
35. Klein NP and Schneider RJ: Activation of Src family kinases by hepatitis B virus HBx protein and coupled signaling to Ras. Mol Cell Biol 17: 6427-6436, 1997.
36. Koike K, Tsutsumi T, Fujie H, Shintani Y and Kyoji M: Molecular mechanism of viral hepatocarcinogenesis. Oncology 62 (suppl 1): 29-37, 2002.

ll J, Wellbrock C, Dexter TJ, Roberts K, Marais R and
g CR: The Brn-2 transcription factor links activated
BRAF to melanoma proliferation. Mol Cell Biol 24: 2923-2931, 2004.
38. Hingorani SR, Jacobetz MA, Robertson GP, Herlyn M and Tuveson DA: Suppression of BRAF(V599E) in human melanoma abrogates transformation. Cancer Res 63: 5198-5202, 2003.
39. Monia BP, Sasmor H, Johnston JF, Freier SM, Lesnik EA, Muller M, Geiger T, Altmann KH, Moser H and Fabbro D: Sequence-specific antitumor activity of a phosphorothioate oligodeoxyribonucleotide targeted to human C-raf kinase supports an antisense mechanism of action *in vivo*. Proc Natl Acad Sci USA 93: 15481-15484, 1996.
40. Broustas CG, Gokhale PC, Rahman A, Dritschilo A, Ahmad I and Kasid U: BRCC2, a novel BH3-like domain-containing protein, induces apoptosis in a caspase-dependent manner. J Biol Chem 279: 26780-26788, 2004.
41. Kumar D, Sakabe I, Patel S, Zhang Y, Ahmad I, Gehan EA, Whiteside TL and Kasid U: SCC-112, a novel cell cycle-regulated molecule, exhibits reduced expression in human renal carcinomas. Gene 328: 187-196, 2004.
42. Haddad B, Pabon-Pena C, Young H and Sun WH: Fine mapping of STAT1 gene by FISH and radiation hybrids. Cytogenet Cell Genet 83: 58-59, 1998.
43. Pan WJ, Pang SZ, Huang T, Guo HY, Wu D and Li L: Characterization of function of three domains in Dishevelled-1: DEP domain is responsible for membrane translocation of Dishevelled-1. Cell Res 14: 324-330, 2004.
44. Widmann C, Gibson S and Johnson GL: Caspase-dependent cleavage of signaling proteins during apoptosis: A turn-off mechanism for anti-apoptotic signals. J Biol Chem 273: 7141-7147, 1998.
45. Hwang A, McKenna WG and Muschel RJ: Cell cycle-dependent usage of transcriptional start sites, a novel mechanism for regulation of cyclin B1. J Biol Chem 273: 31505-31509, 1998.
46. Bolognese F, Wasner M, Dohna CL, Gurtner A, Ronchi A, Muller H, Manni I, Mossner J, Piaggio G, Mantovani R and Engeland K: The cyclin B2 promoter depends on NF-Y, a trimer whose CCAAT-binding activity is cell-cycle regulated. Oncogene 18: 1845-1853, 1999.
47. Lange-zu Dohna C, Brandeis M, Berr F, Mossner J and Engeland K: A CDE/CHR tandem element regulates cell cycle-dependent repression of cyclin B2 transcription. FEBS Lett 484: 77-81, 2000.
48. Wasner M, Haugwitz U, Reinhard W, Tschop K, Spiesbach K, Lorenz J, Mossner J and Engeland K: Three CCAAT-boxes and a single cell cycle genes homology region (CHR) are the major regulation sites for transcription from the human cyclin B2 promoter. Gene 312: 225-237, 2003.
49. Laird AD, Morrison DK and Shalloway D: Characterization of Raf-1 activation in mitosis. J Biol Chem 274: 4430-4439, 1999.
50. Hayne C, Tzivion G and Luo Z: Raf-1/MEK/MAPK pathway is necessary for the G2/M transition induced by nocodazole. J Biol Chem 275: 31876-31882, 2000.
51. Zhou BB and Elledge SJ: The DNA damage response: putting checkpoints in perspective. Nature 408: 433-439, 2000.
52. Rouse J and Jackson SP: Interfaces between the detection, signaling, and repair of DNA damage. Science 297: 547-551, 2002.
53. Shiloh Y: ATM and related protein kinases: safeguarding genome integrity. Nat Rev Cancer 3: 155-168, 2003.
54. Gottlieb TM and Jackson SP: The DNA-dependent protein kinase: requirement for DNA ends and association with Ku antigen. Cell 72: 131-142, 1993.
55. Carson CT, Schwartz RA, Stracker TH, Lilley CE, Lee DV and Weitzman MD: The Mre11 complex is required for ATM activation and the G2/M checkpoint. EMBO J 22: 6610-6620, 2003.
56. Kitagawa R, Bakkenist CJ, McKinnon PJ and Kastan MB: Phosphorylation of SMC1 is a critical downstream event in the ATM-NBS1-BRCA1 pathway. Genes Dev 18: 1423-1438, 2004.